Molecular Crystals and Liquid Crystals Incorporating Nonlinear Optics

Publication details, including instructions for authors and subscription information:
http://www.tandfonline.com/loi/gmcl17

Electrooptics of a Nematic Liquid Crystal in a Spatially Nonuniform Field

Vladimir Chigrinov [a]

[a] Organic Intermediates, & Dyes Institute, Moscow, USSR

Version of record first published: 20 Apr 2011.

To cite this article: Vladimir Chigrinov (1990): Electrooptics of a Nematic Liquid Crystal in a Spatially Nonuniform Field, Molecular Crystals and Liquid Crystals Incorporating Nonlinear Optics, 179:1, 71-91

To link to this article: http://dx.doi.org/10.1080/00268949008055357

Mol. Cryst. Liq. Cryst., 1990, Vol. 179, pp. 71–91
Reprints available directly from the publisher
Photocopying permitted by license only

Printed in the United States of America

ELECTROOPTICS OF A NEMATIC LIQUID CRYSTAL IN A SPATIALLY NONUNIFORM FIELD

VLADIMIR CHIGRINOV
Organic Intermediates & Dyes Institute,
Moscow, USSR

Abstract The paper presents an original theoretical approach to electrooptical effects in a spatially nonuniform field. Various types of initial orientation of LC - planar, homeotropic and twist - as well as different forms of a spatially nonuniform field, including a harmonic field, a flat capacitor edge field, a point potential field etc. are investigated. The LC layer sensitivity and resolution are shown to be significantly determined by the LC material physical parameters. The obtained results could be useful in designing various electrooptical devices in which LC optical properties vary in accordance with the spatially nonuniform distribution of the exciting electric field.

INTRODUCTION

For many cases of practical importance the optical response of a nematic Liquid Crystal (LC) depends on the distribution of a spatially nonuniform electric field. For instance, electrooptical effects in a spatially nonuniform field occur in Photoconductor-Liquid Crystal[1-3] (PC-LC) structures, pyroelectric-LC structures[4,5] matrix-LC modulators-controlled transparencies[6,7] as well as in LC flaw detection of IC dielectric layers and visualization of contact windows in dielectric films[8,9] and so on. By analysing an LC elect-

rooptical behaviour in a nonuniform field one can estimate different characteristics of the LC layer, in particular, sensitivity (i.e. the intensity of optical response at a given voltage), spatial resolution (the optic image capability to distinguish delicate details of a spatially nonuniform electric distribution) etc.

Till recently there have been actually no works on investigations of LC electrooptical properties in a spatially nonuniform field due to cumbersome calculations involved and their experimental verification difficulties. Now a growing interest of experimentors[1-9] towards this problem is observed; anyhow theoretical investigations are practically absent.

LIQUID CRYSTAL PLANAR ORIENTATION. PHASE CONTRAST

Optical characteristics of a planar oriented nematic LC in a nonuniform electric field are discussed in[10-11]. The nonuniform electric field

$$E = -\,\mathrm{grad}\, U(x,z) = (E_x, 0, E_z) \qquad (1)$$

in this case occurs in the vicinity of one of the LC cell substrates:

$$U|_{z=L} = U_0(x), \qquad (2)$$

while on another substrate a zero potential is maintained:

$$U|_{z=0} = 0 \qquad (3)$$

Suppose the director bias from the initial planar orientation along x-axis,

$$\bar{n} = (\cos\Theta, 0, \sin\Theta) \sim (1, 0, \Theta) \qquad (4a)$$

or along y-axis,

$$\bar{n} = (\cos\Theta\sin\Psi, \cos\Theta\cos\Psi, \sin\Theta) \sim (\Psi, 1, \Theta) \quad (4b)$$

is small, $|\Psi|, |\Theta| \ll 1$. Then a nonuniform potential, $U(x,z)$, inside the LC layer ($0 \leq z \leq L$) satisfies the Laplace equation:

$$\frac{\partial^2 U}{\partial x'^2} + \frac{\partial^2 U}{\partial z'^2} = 0 \quad (5)$$

with the boundary conditions of (2), (3), where $x' = (\varepsilon_\perp / \varepsilon_\parallel)^{1/2} \cdot \frac{x}{L}$ for the case (a) and $x' = x/L$ for the case (b), $z' = z/L$, $\varepsilon_\parallel$ and $\varepsilon_\perp$ being LC dielectric constants (Figure 1).

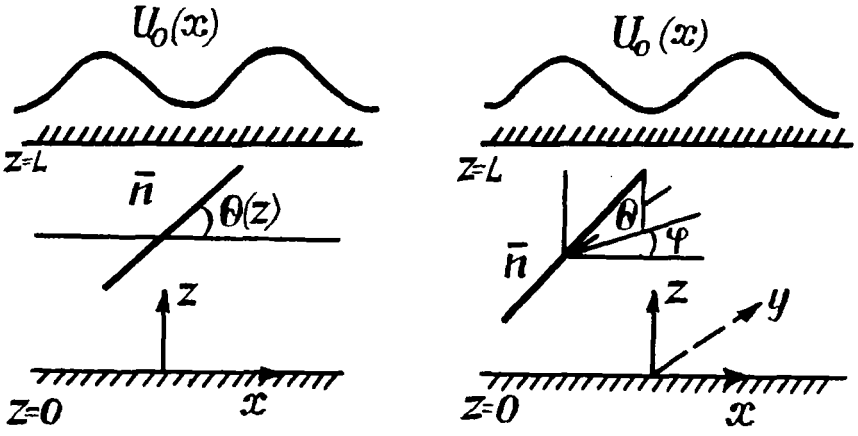

(a) (b)

FIGURE 1. Two possible planar director orientations in a nonuniform field

Several solutions of (5), (2), (3) for various potential values, $U_0(x')$, are summarized in Table 1.

TABLE 1 Spatially nonuniform potential, U, inside an LC layer

$U_0(x')$	$U(x',z')$	Type of Field	
$V_0(1+m\cdot\sin\omega_s x')$ $V_0, m, \omega_s = const.$	$V_0\left(z'+m\cdot\frac{\sin\omega_s x'\cdot sh\omega_s z'}{sh\omega_s}\right)$	Harmonic law[11]	(6)
V_0, $\tilde{x}\le 0$ 0, $\tilde{x}>0$	$\frac{V_0}{\pi}\cdot a(\tilde{x},\tilde{z})$, $\tilde{x}-1=\beta+\exp(\beta)\cdot\cos\alpha$ $\tilde{z}=\alpha+\exp(\beta)\cdot\sin\alpha$, $0\le\alpha\le\pi$, $-\infty<\beta<\infty$, $\tilde{x}=\pi x'+1$, $\tilde{z}=\pi z'$	A flat capacitor edge field[10]	(7)
$\int_0^\infty a(\xi)\cos\xi x'd\xi$	$\int_0^\infty a(\xi)\cdot\frac{\cos\xi x'\cdot sh\xi z'}{sh\xi}d\xi$	The arbitrary even potential expandable into a Fourier series[11]	(8)

The LC-director bias from the initial planar orientation in a nonuniform field leads to intensity modulation, I,(or the amplitude contrast) of the light passed through an LC cell in crossed polaroids in the form of[1]

$$I = I_0 \cdot \sin^2 2\varphi_0 \cdot \sin^2 \Delta\Phi/2, \qquad (9)$$

where I_0 is the intensity of the linearly polarized light incident on the LC cell, φ_0 is an angle between the polarization vector of the incident light and the LC-director.

$$\Delta\Phi = \frac{2\pi}{\lambda} L \Delta n \qquad (10)$$

is phase difference (phase contrast) between an ordinary beam with the birefringence value of $n_\perp$ and an extraordinary one with the birefringence value of $n_\parallel$:

$$n = n_\parallel n_\perp (n_\parallel^2 \sin^2\Theta + n_\perp^2 \cos^2\Theta)^{-1/2},$$
$$\Delta n = 1/L \cdot \int_0^L (n - n_\perp) dz \qquad (11)$$

is birefringence, L is the LC layer thickness. Substituting $\Theta(x', z)$ into (11) and integrating over z-coordinate, we obtain distribution of phase contrast, $\Delta\Phi(x')$, (10) and intensity of the light passed through I(x')(9) in the region of the field nonuniformity variation. We note that in approximation of the LC-director small deformations ($|\Theta| \ll 1$) the phase contrast according to (10)-(11) will be

$$\Delta\Phi \sim \Delta\Phi_{max} + \delta,$$
where $$\Delta\Phi_{max} = \frac{2\pi}{\lambda} L (n_\parallel - n_\perp), \quad \delta = -\frac{\pi L}{\lambda} n_\parallel \left(\frac{n_\parallel^2}{n_\perp^2} - 1\right) \langle\Theta^2\rangle, \qquad (12)$$
$$\langle\Theta^2\rangle = 1/L \cdot \int_0^L \Theta^2(x', z) dz$$

is an average square of director bias angle along the LC layer[1].

Let us consider variation of amplitude $I(x')$ and phase $\delta(x')$ contrast for various types of spatially nonuniform field. For the harmonic potential the phase contrast, δ, is a periodical function x' with a period of $T_s=\frac{2\pi L}{\omega_s}$ (Figure 2). The phase contrast curve, $\delta(x')$, during one spatial voltage period, $U_o(x')$, has two maxima corresponding to the maximal value of the $\frac{\partial U_o}{\partial x'}$ derivative, and two minima in which $\frac{\partial U_o}{\partial x'}=0$ (Figure 2). The phase contrast amplitude increases as $\beta'=\frac{K_{33}\varepsilon_\perp}{K_{11}\varepsilon_{||}}$ decreases and the external field, $\delta\sim V_o^4$, grows. Such a law is characteristic of an LC dielectric destabilization. Dependence of phase contrast on spatial frequency, ω_s, will be discussed later.

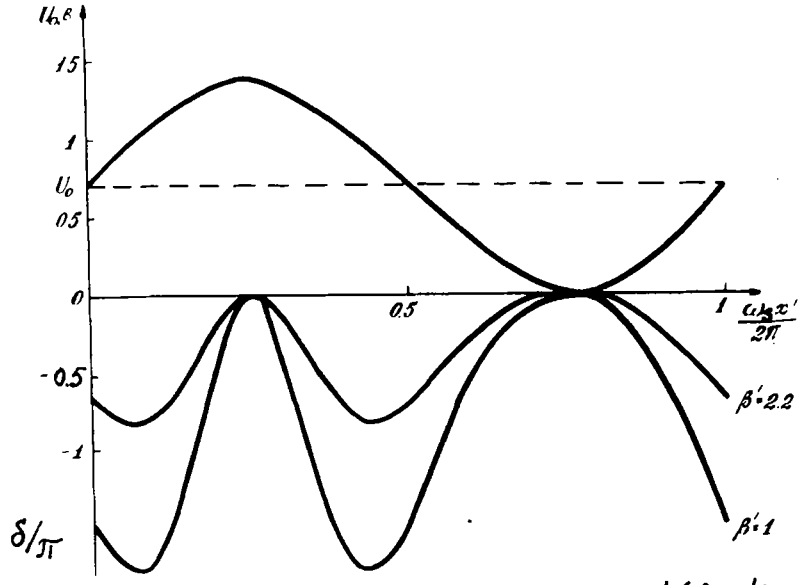

FIGURE 2. The LC phase contrast, $\delta(\frac{\omega_s x'}{2\pi})/\pi$, vs spatial frequency, $\frac{\omega_s x'}{2\pi}$. On top: harmonic potential (6), $V_o=0.7$ V, m=1, L=20μ, $\lambda=0.63\mu$, $n_{||}=1.654$, $n_\perp=1.509$, $K_{11}=0.675\cdot10^{-6}$dyne, $\varepsilon_{||}=31$, $\varepsilon_\perp=9.26$, $\beta'=K_{33}\varepsilon_\perp/K_{11}\varepsilon_{||}$.

The phase contrast shown in Figure 2 also increases with modulation depth (m) of the driving voltage (6).

Variation of phase contrast, $|\delta|/\pi$, from maximum $|\delta|/\pi = 1$ to $\delta = 0$ was numerically calculated for the potential of the (7) type induced by a semi-infinite flat capacitor edge and was compared with the experimental one for two different LC layer thicknesses, namely: L = 20μ and L = 44μ[10] (Figure 3).

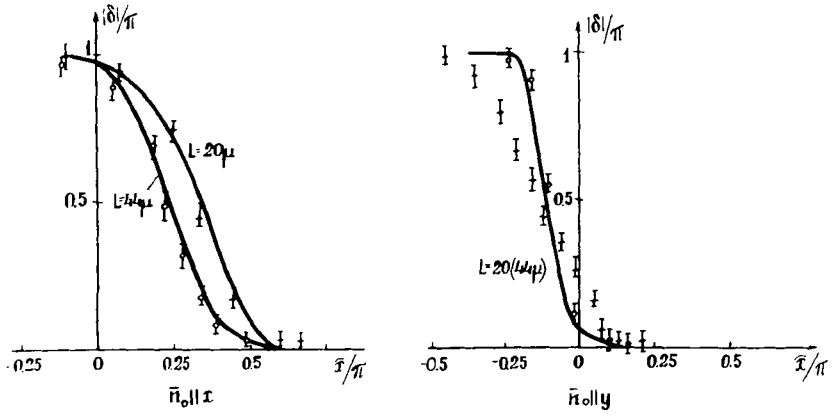

FIGURE 3. Phase contrast distribution near the "flat capacitor edge" for two different planar LC orientations $\bar{n}_0 : \bar{n}_0 \parallel x$ (perpendicular to the capacitor edge) and $\bar{n}_0 \parallel y$ (parallel to the capacitor edge). The solid lines indicate the calculated curves; (o),(×) denote experimental data for L=44μ and L=20μ, respectively.[10] The calculated parameters of[10] are as follows: $\varepsilon_{\parallel}=31$, $\varepsilon_{\perp}=9.26$, $K_{11}=0.765\cdot10^{-6}$, $K_{22}=1.05\cdot10^{-6}$, $K_{33}=1.51\cdot10^{-6}$, $n_{\perp}=1.509$, $n_{\parallel}=1.654$ CGSE units.

The LC layer was selected such as to provide minimum intensity of the transmitted light at zero field:

$$\Delta\Phi_{max} = 2\pi K, \quad K = 0, \pm 1, \pm 2, \ldots$$

In this case one could consider $I = I_o \cdot \sin^2 \delta/2$ and relate phase contrast variation directly with intensity variation $I(|\delta|/\pi = 1) = I_o$, $I(\delta = 0) = 0$. Phase contrast was numerically calculated[10] for LC planar orientation both perpendicular (4a) and parallel (4b) to the flat capacitor edge. Maximal deviations of the numerically calculated phase contrast curve from the experimental one at the length $L = 44\,\mu$ did not exceed 12%. As the length decreased to $L = 20\,\mu$, the deviation increased. This fact can be explained by limited applicability of LC small deformations model used. The smaller the LC layer thickness is, the larger director bias angles must be in order to achieve a fixed value of the phase contrast, $\frac{|\delta|}{\pi} = 1$.

Figure 3 demonstrates spatial dependences of the phase contrast in the transient region for two cases of the director planar orientation relative to the voltage variation axis (x-axis). It can be seen that in case of the LC orientation along y-axis ($\bar{n}_o \| y$) the transient region width is significantly smaller than in case of the LC orientation along the potential axis x ($\bar{n}_o \| x$). Thus the phase contrast variation in the transient region (near the flat capacitor edge) in case of LC planar orientation along x-axis (perpendicular to the capacitor edge) in fact determines a spatial resolution of the given LC structure. As can be seen

from Figure 3, for x-orientation of LC-director the phase contrast variation region extends to the distance of $\tilde{x}_1 \sim 0.1$ under the electrode and to the distance of $\tilde{x}_2 \sim 0.5$ from the electrode edge. Thus, according to (7) the transient region width, $\tilde{x} = \pi(\tilde{x}_1 + \tilde{x}_2)L$ is about double thickness of the LC layer.

HOMEOTROPIC ORIENTATION OF LIQUID CRYSTAL. THE ROLE OF FLEXOELECTRIC EFFECT

Normally, when describing the LC behaviour in a nonuniform field it is implied that the director reorientation takes place due to the effect of a destabilizing moment proportional to $\delta f_\varepsilon / \delta \bar{n}$, where $f_{\varepsilon_a} = -\frac{\varepsilon_a}{4\pi}(\bar{E}\bar{n})^2$ (ε_a - dielectric anisotropy) is a contribution to the free LC energy.[6] Anyhow, the LC response to a spatially nonuniform electric field could be induced by a flexoelectric effect.[11] In this case the destabilizing moment is proportional to $\delta f_e / \delta \bar{n}$, where $f_e = -(e_{11}\bar{n}\bar{E}\,div\,\bar{n} + e_{33}[rot\,\bar{n} \times \bar{n}]\cdot\bar{E})$ is the corresponding contribution to the free energy, e_{11} and e_{33} are flexoelectric coefficients. For

$$|\bar{E}| \ll \frac{4\pi(e_{11}+e_{33})q}{\varepsilon_a}, \qquad (13)$$

where q - is a director deformation wave vector, the flexoelectric effect fully determines all the electrooptical characteristics of LC in a nonuniform field. We investigated a general case of flexoelectric and dielectric destabilization of a homeotropically oriented LC in a nonuniform field varying according to a harmonic law (6).[9,11-13]

In approximation of small director deviations θ from the homeotropic orientation we have:

$$\bar{n} = (\sin\theta, 0, \cos\theta) \sim (\theta, 0, 1), \quad |\theta| \ll 1 \qquad (14$$

The equilibrium condition for three torques - elastic dielectric and flexoelectric - takes the form

$$K_{33}\frac{\partial^2\theta}{\partial z^2} + K_{11}\frac{\partial^2\theta}{\partial x^2} + e_{33}\frac{\partial E_z}{\partial z} + e_{11}\frac{\partial E_x}{\partial x} - \frac{\varepsilon_a}{4\pi}E_x E_z = 0, \qquad (1$$

where $\bar{E} = (E_x, 0, E_z)$ is a nonuniform electric field, K_{11} and e_{11} are LC elastic and flexoelectric moduli, respectively. On the LC layer boundary at z = 0,L it also necessary to consider the surface polarization, m_p, and the substrate-LC anchoring energy, W_o:

$$\left\{K_{33}\frac{\partial\theta}{\partial z} - E_x(e_{33} - m_p) \pm W_o\theta\right\}_{z=L,0} = 0 \qquad (1$$

In[12,14] an average square of deformation, $\langle\theta^2\rangle$, obtained from (15),(16) is taken as an LC layer diffraction modulation characteristic (a function representi a relative transmission efficiency of various image spatial frequencies). The LC layer resolution and sensitivity are characterized by the magnitude of the spatial frequency, w_{max}, for which the value of $\langle\theta$ is maximal and the proper value of this maximum is $\langle\theta^2\rangle_{max}$ accordingly.

Figure 4 demonstrates the dependences of the Relative Modulation Characteristic (RMC) $i_1(\omega_s) = \langle\theta^2\rangle/\langle\theta^2\rangle_{max}$ on reduced LC-substrate anchoring energy, $a_w = \frac{W_o L}{K_{33}}$. It can be seen that with rise of a_w the curve $i_1(\omega_s)$ becomes smoother and its maximum shifts towards larger values of ω_s. Note that for low anchoring value $a_w \simeq 0.5$ the L deformation amplitude, $\langle\theta^2\rangle_{max}$ drastically increases (F gure 4), so the linear model of the effect we assumed in (15),(16) becomes invalid. For anchoring energies

$a_w \gtrsim 5$ the curve has an inflection and the shape of the $i_1(w_s)$ curve starts to undergo the opposite change (Figure 4). At $a_w \gtrsim 150$ the RMC, $i(w_s)$, comes to the saturation point and further varies no more.

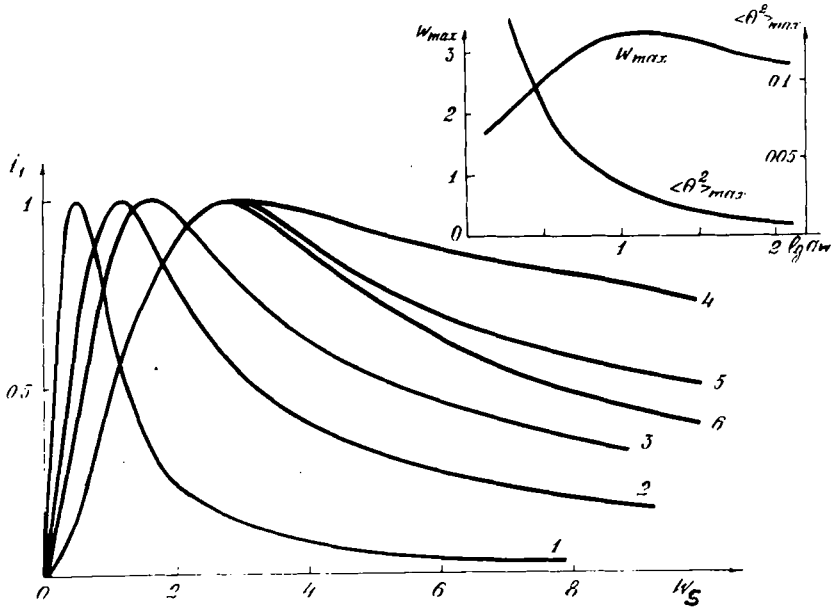

FIGURE 4. Relative Modulation Characteristic (RMC), $i_1(w_s)$, of LC vs electric field spatial frequency, w_s for different LC-substrate reduced anchoring energies a_w. For Curve 1 the anchoring strength coefficient is $a_w = 0.133$ ($W_s = 10^{-4}$ erg/cm^2); 2: $a_w = 0.665$ ($W_s = 5 \cdot 10^{-4}$ erg/cm^2); 3: $a_w = 1.33$ ($W_s = 10^{-3}$ erg/cm^2); 4: $a_w = 6.65$ ($W_s = 5 \cdot 10^{-3}$ erg/cm^2); 5: $a_w = 66.5$ ($W_s = 5 \cdot 10^{-2}$ erg/cm^2); 6: $a_w = 133$ ($W_s = 0.1$ erg/cm^2). The LC parameters are as follows:[12] $K_{11} = 10^{-6}$, $K_{33} = 1.5 \cdot 10^{-6}$, $e_{11} = 10^{-4}$, $e_{33} = m_p = 2.8 \cdot 10^{-4}$, $\varepsilon_\perp = 5.6$, $\varepsilon_{//} = 6.6$ CGSE units, $L = 20^p$, $V_0 = 1$ V, $m = 0.5$.

The plots given in the right top corner of Figure 4 show dependences of ω_{max} and $\langle\theta^2\rangle_{max}$ on $\lg a_w$.

The modulation characteristic depends on the LC dielectric anisotropy, $\varepsilon_a=\varepsilon_{11}-\varepsilon_\perp$. The "isotropic" point, $\varepsilon_a=0$, is not singular, as the LC-director in the nonuniform electric field reorients due to the flexoelectric effect. For the positive ε_a values the dielectric torque, induced by a nonuniform field, is added to the flexoelectric one, the result being a growth of the maximal deformation, $\langle\theta^2\rangle_{max}$. With the decrease of ε_a the RMC maximum, ω_{max}, is shifted towards the larger values, i.e. the spatial resolution of the structure increases at low LC dielectric anisotropy, ε_a, values.

The LC splay and bend elastic moduli, K_{11} and K_{33}, also play an important role in determination of an LC layer sensitivity and resolution in a spatially nonuniform electric field. The lower the elastic moduli magnitudes, the larger is the LC deformation amplitude at a given V_o voltage (LC layer sensitivity). This effect is particularly evident for low K_{11} values. The decrease of K_{11} leads to a marked improvement of the LC layer spatial resolution. On the other hand, it would be unreasonable to drastically decrease the K_{33} value, as in this case the LC resolution, ω_{max}, becomes worse. Consequently, we come to the conclusion, that optimal sensitivity and resolution of an LC layer with a homeotropic alignment can be achieved at $K_{33}\lesssim 10^{-6}$ dyne and the highest possible elastic moduli ratio, K_{33}/K_{11}.

A.V.Parfenov[12,14] experimentally verified the dominating influence of flexoelectric effect on a homeotropic LC deformation in a spatially nonuniform harmonic electric field. Measurements were made in a photoconductor-LC structure using the holographic technique. The controlling light signal was formed by the interferometric method and was observed to undergo a spatial harmonic change and to be transformed into a harmonic driving voltage distribution on the LC layer. In the experiment a relative intensity I_1/I_0 of the reading-off light first diffraction maximum on the deformed LC periodic structure was measured vs spatial frequency, ω_s, of the controlling optoelectronic signal. The amplitude, V_0, and the modulation depth, m, of the nonuniform electric field were chosen small to provide the condition of low LC deformation (the first order diffraction intensity did not exceed 8-10% of the zero order intensity). The signal spatial frequency variation was performed using the Michelson interferometer.

The important role of flexoelectric effect for LC deformations in a nonuniform electric field can be experimentally proved as follows.

1. The "isotropic" point, $\varepsilon_a=0$, where the dielectric torque is zero, has no specific features. The experiment with an LC having $\varepsilon_a=0$[12] gives the same qualitative modulation characteristics of $i_1(\omega_s)$ as for LCs having $\varepsilon_a \neq 0$.

2. In an AC electric field with the time frequency, ω_t, at a low V_0 amplitude value the optical signal of I_1/I_0 modulates with the frequency

of $2\omega_t$, the constant signal component being absent. This means that the director bias angle is directly proportional to the applied voltage and that is characteristic of a flexoelectric effect. As the electric field amplitude in optical modulation I_1/I_0 increases, there appears a frequency component of $4\omega_t$, typical for the Fredericks effect.[12]

Finally we would like to point out that by the type of a modulation curve, $i_1(\omega_s)$, one can estimate the anchoring energy of a homeotropic NLC. Thus, according to our evaluation the anchoring energy of a homeotropic NLC containing about 1 % of lecithin amounts to approximately $5 \cdot 10^{-4}$ erg/cm^2, while in the absence of lecithin it amounts to about 10^{-4} erg/cm^2.

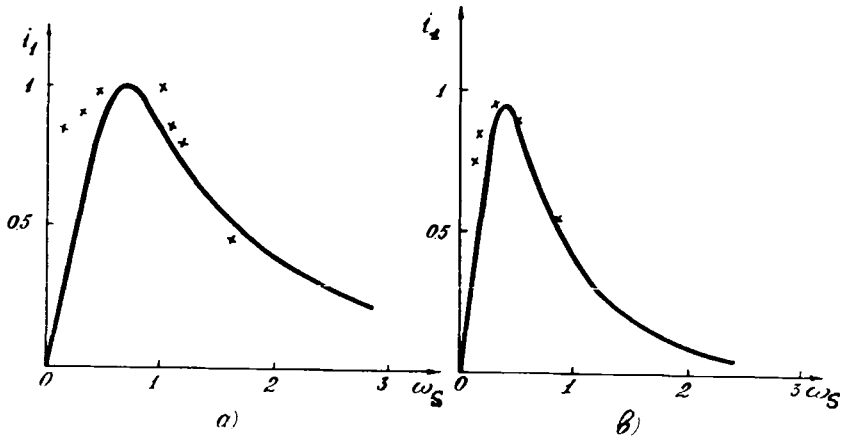

FIGURE 5. Comparison of the LC modulation curves obtained by different procedures: a) treating the substrate by lecithin; b) spontaneous homeotropic orientation.(x) indicate experimental data, solid lines represent the calculated values.[11]

We assume $L=5\mu$, $\varepsilon_{\parallel}=5.47$, $\varepsilon_{\perp}=5.35$, $\varepsilon_a=0.02$, the other LC parameters being the same as in Figure 4. The anchoring energy values, $W_0 = 5\cdot10^{-4}$ erg/cm^2 (a) and $W_0=10^{-4}$ erg/cm^2 (b) are obtained by the LMS method (Figure 5).

HOMEOTROPIC LC IN A RADIAL-SYMMETRICAL NONUNIFORM ELECTRIC FIELD. OPTICAL LC VISUALIZATION OF SURFACE DEFECTS

Let the nonuniform electric potential near an LC substrate be presented in a cylindrical coordinate system (ρ, φ, z) as follows:[9]

$$U|_{z=L} = U_0(\rho) = \begin{cases} V_0, & \rho \le a_0 \\ 0, & \rho > a_0, \end{cases}$$

$$U|_{z=0} = 0$$

This type of a nonuniform electric field occurs, for instance, in those cases when the applied to the LC field is zero everywhere except for a finite circle with a radius of a_0 being a surface defect.[8,9]

Figure 6 shows the averaged LC deformation proportional to the relative phase contrast in the field nonuniformity region.[9] The deformation is seen to be zero at the centre of the defect and reaches its maximum on its edge, where the field nonuniformity is most evident. The maximum amplitude of the phase contrast at a given voltage is proportional to the sensitivity of the LC surface defect optical visualization method.[8,9] At the same time the steepness of the phase contrast curve in the vicinity of the defect defines the method resolution, i.e. its capability to distin-

guish closely located defects. As can be seen from Figure 6, the sensitivity is maximal for $\beta' = K_{33}\varepsilon_a / K_{11}\varepsilon_{\parallel} = 1$, while the resolution deteriorates with decrease of β'. The magnitude of the deformation, $\langle\theta^2\rangle$, (or sensitivity) grows proportional to a square of the coefficient, $A_f \sim \frac{e_{11} e_{33}}{K_{11}}$ and at $V_0 < \frac{4\pi(e_{11}+e_{33})}{\varepsilon_a}$ is entirely determined by a flexoelectric effect in a nonuniform electric field.

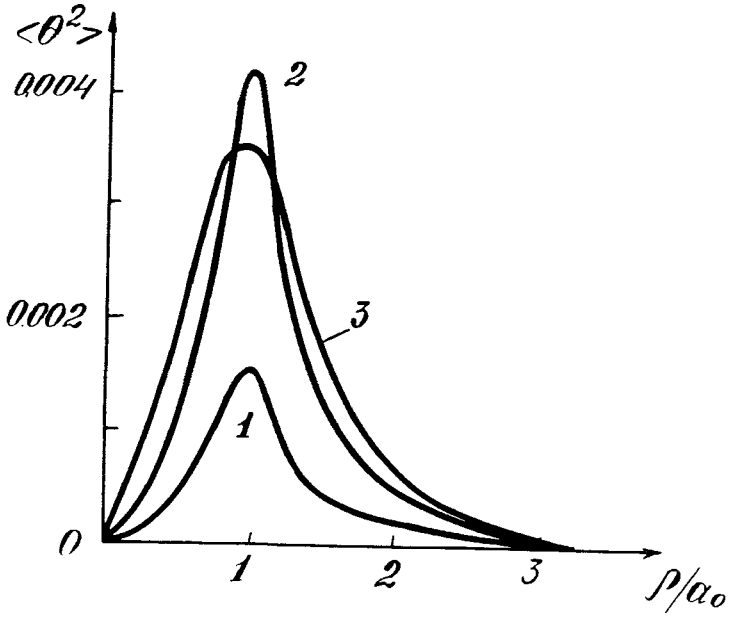

FIGURE 6. Averaged LC deformation, $\langle\theta^2\rangle$, in the vicinity of the surface defect region with the radius of a_0. ρ/a_0 is a relative distance from the defect centre. The numeric calculations were made for the following LC parameters: $e_{11}=e_{33}=10^{-4}$, $K_{11}=10^{-6}$ CGSE units, $a_0/L=0.05$, $V_0=3$ V. For Curve 1: $\beta' = \frac{K_{33}\varepsilon_a}{K_{11}\varepsilon_{\parallel}} = 9.6$; 2: $\beta' = 1$; 3: $\beta' = 0.24$.

LC TWIST STRUCTURE. OPTICAL TRANSFER FUNCTION AND RESOLUTION

Calculations of LC twist structure resolution in a nonuniform field are very cumbersome and for this reason have not been attempted till recently. The direct minimization algorithm of LC free energy functional proposed by us together with S.N.Levov et al. stimulated progress in the field.[11,13] The obtained Optical Transfer Function (OTF) of a twist structure can be used in modelling of linear optical systems containing an LC twist cell as a unit.

The results of the calculation of the twist structure resolution depending on the LC physical parameters and layer thickness are summarized in Table 2.

TABLE 2 Resolution of LC twist structure, ν_R.

Item No.	LC parameter	Resolution		
1.	Layer thickness, L,	3	6	12
	ν_R (line/mm)	54	26	12
2.	Relative dielectric anisotropy,	0.1	0.5	
	ν_R (line/mm), L=3	65	54	
3.	Optical anisotropy,	0.1	0.2	0.3
	ν_R (line/mm), L=6	27	26	24
4.	Elastic moduli ratio, K_{33}/K_{11},	1	1.5	2.5
	ν_R (line/mm), L=3	54	52	48

The following average LC parameters are used in

the calculations: $K_{33}/K_{11}=1.26$, $K_{22}/K_{11}=0.85$, $\varepsilon_a/\varepsilon_\perp=0.5$, $\Delta n=0.2$.

Table 2 reveals that the most important parameters affecting spatial resolution of the LC twist structure prove to be the layer thickness, L, and the relative dielectric anisotropy, $\varepsilon_a/\varepsilon_\perp$. The decrease of L or $\varepsilon_a/\varepsilon_\perp$ considerably improves the resolution. The resolution was shown to be practically independent of the elastic moduli ratio, K_{22}/K_{11}, on the range $0.5 \leq K_{22}/K_{11} \leq 1$ which is typical of LC materials.

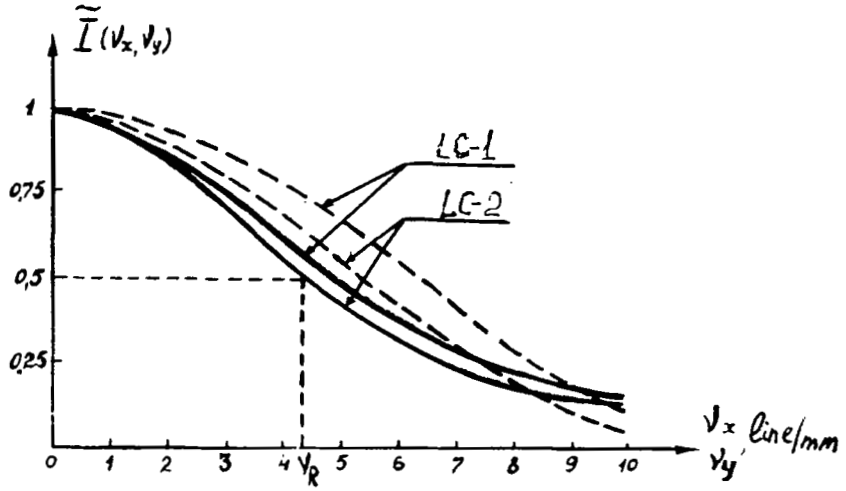

FIGURE 7. Experimental (solid lines) and calculated (dotted lines) absolute values of the twist-structure Optical Transfer Functions. for two LCs: LC-1 and LC-2.[11,13] L=20μ, λ= 3÷5μ. The halfwidth ν_R (line/mm) of the curve indicates the LC spatial resolution.

Figure 7 presents comparative results of experimental and calculated OTFs for two different

LCs:[11,13] LC-1 (the mixture of azoxycompounds) and LC-2 (the mixture of tolanecompounds). In the experiment the output spatial intensity variation of the LC twist-structure (placed between parallel polaroids) was measured as a function of x and y distances from the edge of the transparent electrode, made in the form of a sector (a physical equivalent of the Hewiside function[13]). The subsequently obtained intensity distribution was used for calculation of the twist-structure OTF. The experiment was carried out in the spectral range $\lambda \sim 3 \div 5.5\mu$ for the LC layer thickness $L=20\mu$. It is evident, that the spatial resolution of the LC twist structure obtained in the experiment equals to 4 ÷ 6 line/mm, which is in a qualitative agreement with the theory.

CONCLUSION

A theory for calculation of nematic liquid crystal optical characteristics in a spatially nonuniform electric field is presented. The LC layer sensitivity and resolution are investigated depending on various types of a spatially nonuniform field, the LC physical parameters and its initial orientation, layer thickness and the LC-substrate anchoring energy. An important role of flexoelectric effect in LC electrooptics in a spatially nonuniform field is demonstrated.

The main results are as follows:[10-14]

1. In a spatially nonuniform field an LC is first of all affected by the field coordinate variation rather than the magnitude of the field itself (Figure 2).

2. The extent of the region where the edge effect occurs and which determines the resolution of the homogeneously oriented LC layer is maximal when the director lies in the field nonuniformity variation plane and is about double LC layer thickness in size (Figure 3).

3. The flexoelectric effect contribution to the LC layer deformation is decisive, when the LC dielectric anisotropy, ε_a, is sufficiently low (13).

4. Variating the LC-substrate anchoring energy, W_o, dielectric anisotropy, ε_a, and elastic moduli, K_{11} and K_{33}, it is possible to increase sensitivity and resolution of the LC layer in a spatially nonuniform field (Figure 4).

5. Maximal sensitivity and resolution of the LC material used for visualization of surface defects in an electric field are achieved at $K_{33}/K_{11} = \varepsilon_{\parallel}/\varepsilon_{\perp} = 1$ (Figure 6).

6. A nematic LC twist structure resolution can be improved by decreasing a dielectric anisotropy, ε_a, and an LC layer, L. The LC twist structure resolution is only weakly influenced either by elastic anisotropy, K_{33}/K_{11}, or by optical anisotropy, Δn, (Table 2).

The theoretical results are in a good agreement with the experimental evidence and could be used in selection of optimal LC materials in such

systems as photoconductor-LC and pyroelectric-LC as well as in LC flaw detection etc.

REFERENCES

1. L. M. Blinov, Electro and Magnetooptics of Liquid Crystals (Nauka, Moscow, 1978).
2. A. A. Vasiliev, D. Casasent, I. N. Kompanets, A. V. Parfenov, Spatial Modulators of Light (Radio i Svyaz, Moscow, 1987).
3. C. S. Sexton, SPIE, Liquid Cryst. and Spatial Light Modulat. Mater., 684, 60 (1986).
4. V. P. Vashurin, D. I. Dergachev, I. N. Kompanets, A. V. Parfenov, N. A. Tikhomirova, Preprint 248, (FIAN, Moscow, 1985).
5. A. R. Mordukhaev, V. N. Chirkov, V. E. Hutorskiy, B. S. Gurevich, USSR Conference on Optics of Liquid Crystals, Abstracts (Moscow, 1987), p. 197.
6. A. A. Vasiliev, Candidate Theses (FIAN, Moscow, 1980).
7. D. G. Sikharulidze, G. S. Chilaya, Image Transducers on MDM - Electrooptical Material Type (Radio i Svyaz, Moscow, 1986).
8. A. E. Rubtsov, G. E. Nevskaya, Electronic Technical Review, 8, No.1 (1986).
9. G. E. Nevskaya, V. G. Chigrinov, S. F. Dzenis, 4th USSR Liq. Cryst. Conf., Abstracts (Chernigov, 1988), 4, p. 516.
10. V. G. Chigrinov, I. N. Kompanets, A. A. Vasiliev, Molec. Cryst. Liq. Cryst., 55, 193 (1979).
11. V. G. Chigrinov, Doctoral Thesis (Moscow, 1988).
12. V. G. Chigrinov, A. V. Parfenov, 11th Intern. Liq. Cryst. Conf., Berkely, USA, 1986. Abstracts, MA-45.
13. Yu. K. Grusevich, G. A. Beresnev, V. G. Chigrinov, S. N. Levov, 12th Intern.Liq. Cryst. Conf., Freiburg, FRG, 1988, Abstracts, AP-12.
14. A. V. Parfenov, V. G. Chigrinov, ibid, AP-34.